

RESEARCH

Open Access



Hydrogen peroxide enhances transforming growth factor beta-2 induced epithelial–mesenchymal transition of ARPE-19 cells

Brijesh Gelat¹, Pooja Rathaur², Pooja Malaviya², Binita Patel³, Abhay R. Vasavada² and S. R. Kaid Johar^{1*}

Abstract

Background In the pathophysiology of the retina, the epithelial–mesenchymal transition and oxidative stress play key roles. To find a relationship between oxidative stress and diabetic retinopathy or proliferative retinopathy, we used an in-silico approach. We also used an in vitro investigation to examine the synergistic effect of transforming growth factors-β2 (TGFβ2) and hydrogen peroxide (H₂O₂) on the epithelial–mesenchymal transition (EMT) of ARPE-19 cells, analyzing cell survival, cell migration by wound healing, and expression epithelial–mesenchymal transition markers at the protein and mRNA levels.

Results For 24 h, human retinal pigment epithelial cells (ARPE-19) were cultured in standard conditions and subjected to various concentrations of TGFβ2, H₂O₂, and their combinations. According to a bioinformatics study, signaling pathways including hypoxia-inducible factor (HIF-1), forkhead box O (FoxO), phosphoinositide-3-kinase (PI3K-Akt), and transforming growth factors-β (TGFβ-signaling), both growth factors and oxidative stress-associated proteins play a significant role in the development of retinopathies. In vitro studies showed that oxidative stress induced by H₂O₂ and TGFβ2 enhances the epithelial–mesenchymal transition of ARPE-19 cells.

Conclusions Hydrogen peroxide enhances the TGFβ2-mediated epithelial–mesenchymal transition of human retinal pigment epithelial cells, or at least in cell line ARPE-19 cells.

Keywords Epithelial–mesenchymal transition, Human retinal pigment epithelial cells, Transforming growth factors-β2, Hydrogen peroxide, Oxidative stress, ARPE-19

*Correspondence:

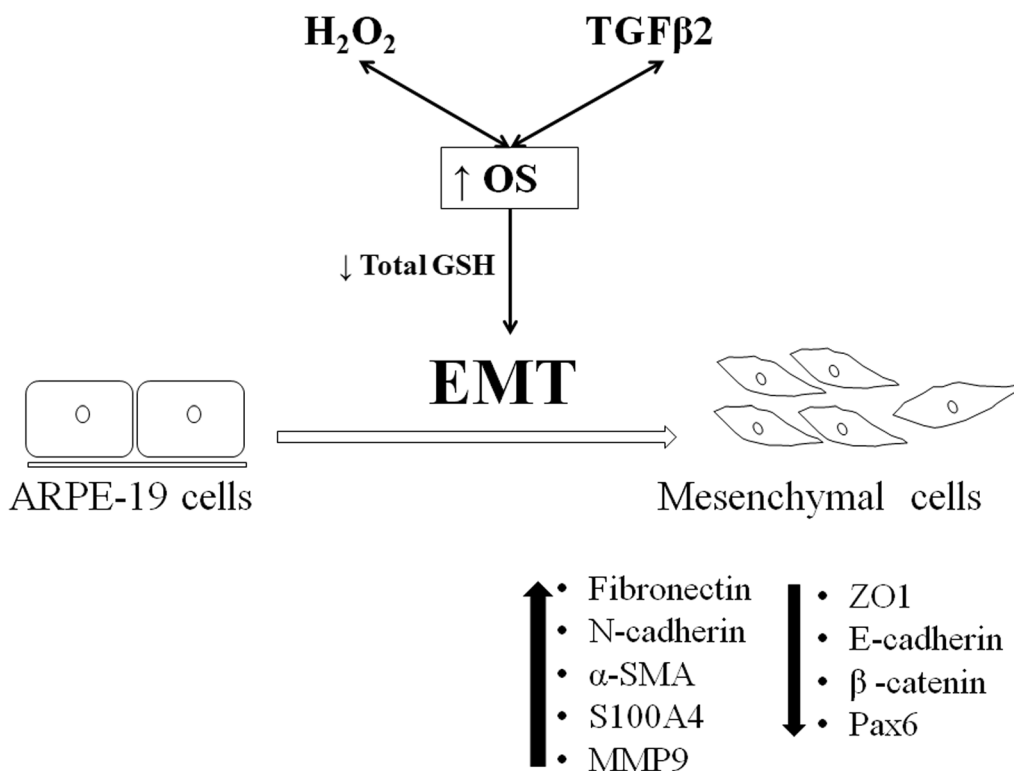
S. R. Kaid Johar
qaidjohar110@gmail.com

Full list of author information is available at the end of the article



© The Author(s) 2023. **Open Access** This article is licensed under a Creative Commons Attribution 4.0 International License, which permits use, sharing, adaptation, distribution and reproduction in any medium or format, as long as you give appropriate credit to the original author(s) and the source, provide a link to the Creative Commons licence, and indicate if changes were made. The images or other third party material in this article are included in the article's Creative Commons licence, unless indicated otherwise in a credit line to the material. If material is not included in the article's Creative Commons licence and your intended use is not permitted by statutory regulation or exceeds the permitted use, you will need to obtain permission directly from the copyright holder. To view a copy of this licence, visit <http://creativecommons.org/licenses/by/4.0/>.

Graphical abstract



1 Background

The retinal pigment epithelium (RPE) cells are a single layer of highly polarized cells located between the choroid and photoreceptors. Each adult human eye has around 3.5 10⁶ cells of the retinal pigment epithelium. Retinal pigment epithelium cells are traditionally assumed to undergo terminal differentiation throughout life [1, 2]. Retinal pigment epithelium cells are essential for maintaining healthy retinal physiology and the different signaling cascades required for optimal vision. They also have a significant impact on the movement of nutrients from the choroid to the inner retinal membranes and the absorption of extra dispersed light to prevent photooxidation [3]. The blood-retinal barrier (BRB), a monolayered cuboidal epithelium held together by cell-cell junctional structures such as tight junctions and adherens junctions, is a function of the retinal pigment epithelium cells in addition to their role in metabolizing retinoid molecules in the visual cycle [4, 5]. Along with maintaining the milieu, the RPE also secretes cytokines that, in some circumstances, might lead to pathological alterations such as macrophage recruitment [6].

In the human body, mesenchymal cells and epithelial cells differ in their characteristics and roles. Expression of junctional complexes and apical-basal polarization are two key characteristics of terminally differentiated epithelial cells. A basal membrane surrounds epithelial cells, separating them from other tissue constituents. Mesenchymal cells, as opposed to epithelial cells, are non-polarized cells with invasive and migrating activity [2, 7, 8]. Many biological processes, including embryogenesis, tissue fibrosis, and cancer metastasis, include the epithelial-to-mesenchymal transition. Loss of cell polarity and adhesion during the transition from epithelial to mesenchymal tissue causes morphological alterations in the cells as well as increased motility and size [9] [10]. Type I EMT occurs in the early phases of embryogenesis, Type II EMT is linked to tissue regeneration and organ fibrosis, and Type III EMT occurs in cancer cells and promotes invasion and metastasis [2, 3, 8]. As mentioned previously, the epithelial-mesenchymal transition is brought on by abnormal stimuli and a modified microenvironment, and it commonly results in tissue or organ fibrosis

[11–15]. A growing body of research demonstrates that various degenerative retinal illnesses cause the retinal pigment epithelial cells to become less differentiated, undergo EMT, and then migrate more easily [16, 17] [3]. Epithelial–mesenchymal transition affects proliferative retinopathy, proliferative diabetic retinopathy, and other degenerative illnesses of the retina [15, 18]. Clinical evidence suggests that macular degenerations and proliferative vitreoretinopathy (PVR) cause retinal pigment epithelial cells to undergo EMT [2, 3, 17]. Loss of vision in age-related macular degeneration (AMD) may come from the breakdown of the BRB, choroidal neovascularization (CNV), and associated exudative fluids invading the subretinal region; aberrant cytokine release may also accelerate disease activity [6].

Oxidative stress is defined as an imbalance between levels of reactive oxygen species and antioxidants [19]. An increase in intracellular reactive oxygen species production can result in oxidative stress [9]. Reactive oxygen species are produced by regular cellular metabolism (mitochondrial electron transport chain) as well as in response to cytokines and environmental stimuli (radiation). Organ fibrosis may be significantly influenced by moderate chronic oxidative stress [20]. Damage caused over time to vital macromolecules by oxidative stress is one of the key factors in age-related diseases. The retina is particularly prone to oxidative stress-induced injury because of its elevated oxygen tension, ongoing exposure to light, and high concentration of polyunsaturated fatty acids (PUFA) [21, 22]. Numerous eye conditions, including proliferative vitreoretinopathy and diabetic retinopathy, as well as macular degenerative retinal diseases, are caused by oxidative stress [6, 23, 24]. One of the reactive oxygen species is hydrogen peroxide, and evidence has revealed that it is more prevalent in the aqueous humor of human eyes with proliferative retinopathies like proliferative diabetic retinopathy and proliferative vitreoretinopathy [25]. Superoxide dismutase, catalase, and glutathione peroxidase have all been found in retinal tissues like retinal pigment epithelium cells and photoreceptors [19, 26, 27].

Transforming growth factor beta (TGF- β), a subclass of cytokines controls many cellular processes, including cell division, proliferation, and differentiation [28–30]. Both oxidative stress/Reactive Oxygen Species (ROS) and transforming growth factor-beta (TGF- β) play crucial roles in health and disease [31]. ROS production can be boosted by TGF- β in both transformed and non-transformed cells. Furthermore, numerous studies have demonstrated that TGF- β can stimulate the production of ROS in various cellular compartments [31, 32]. There is growing evidence to support the idea that ROS induction is the mechanism by which TGF β -induced

EMT is regulated [2, 33]. Particularly during pathological conditions linked to the fibrosis of ocular structures, including retina pigment epithelial cells, TGF β 2 concentration was found to increase [15, 34–36]. Transforming growth factors beta (TGF β) family proteins are essential for the epithelial–mesenchymal transition and associated organ fibrosis, such as proliferative vitreoretinopathy [37, 38].

It is still unknown what causes the epithelial to mesenchymal transition across this continuum. RPE dysfunction is described in this context as the transition from fully differentiated epithelial cells to mesenchymal cells (including the intermediate states). Aging, the breakdown of tight junctions, the buildup of misfolded protein, and inflammation are possible mechanisms underlying RPE dysfunction [2, 3, 16, 17]. Thus, the onset of retinopathies is associated with both the epithelial–mesenchymal transition and oxidative stress. Multiple studies have demonstrated that β 2 exposure causes oxidative stress [15, 31, 39].

We hypothesized that elevated ROS and TGF β together trigger retinal pigment epithelium changes from epithelial to mesenchymal states. This theory was tested in the current work, which looked at the molecular processes behind the epithelial–mesenchymal transitions of the retinal pigment epithelium caused by hydrogen peroxide and TGF β -2. According to this work, TGF β 2-mediated processes connect oxidative stress to epithelial–mesenchymal transitions of the retinal pigment epithelium for the first time. The goal of the current work is to identify shared pathways between epithelial–mesenchymal transition and oxidative stress in retinal pigment epithelium cells using in-silico (bioinformatics) techniques. Additionally, utilizing in vitro studies on the RPE cell line ARPE-19, we investigated how TGF β 2 and H₂O₂-associated factors affected cell migration and the expression of epithelial–mesenchymal transition markers at the cellular, mRNA, and protein levels.

2 Methods

2.1 Materials

ARPE-19, a human retinal pigment epithelial cell line was purchased from American Type Culture Collection (ATCC, Manassas, VA, USA). Dulbecco's modified eagle medium (DMEM/F12) (ThermoFisher, MA), fetal bovine serum (FBS) (ThermoFisher), hydrogen peroxide (Merck), TGF β 2 (Peprotech, USA) were purchased from respective sources. The primary antibodies were purchased from Cell Signaling Technology (CST, Beverly, MA, USA). The nitrocellulose membranes were purchased from Millipore, USA. The bicinchoninic acid

assay (BCA) (Sigma) kit and the chemiluminescence kit were purchased from ThermoFisher (Rockford, IL, USA).

2.2 Identification of oxidative stress and diabetic retinopathy-associated potential genes

The GeneCards database (<https://www.genecards.org>) was used to identify genes associated with oxidative stress based on relevance scores > 10, a cutoff suggesting a considerably high link with oxidative stress. GeneCards is a freely available database that offers in-depth details on predicted and annotated human genes [40]. Proliferative vitreoretinopathy and potential diabetic retinopathy genes (C0011884) were discovered using the DisGeNET database (<https://www.disgenet.org/>). It incorporates knowledge of genetic variations and genes linked to human disease [41]. In addition, the PharmMapper program (<http://www.lilab-ecust.cn/pharmmapper/>) was used to find proteins linked to glutathione.

2.3 Construction and analysis of protein–protein interaction (PPI) networks

At the highest confidence level, protein–protein interaction networks of oxidative stress-associated potential genes, proliferative vitreoretinopathy, and diabetic retinopathy were created using the string database version 11.5 [42]. In order to investigate the relationship between oxidative stress-associated proteins and proliferative vitreoretinopathy as well as diabetic retinopathy, integrated networks were created using the “merge” tool (intersection option was selected) of Cytoscape software version 3.8.2 [43]. Using Database Annotation, Visualization, and Integrated Discovery (DAVID) version 6.8 (<https://david.ncifcrf.gov/>), the proteins of a combined oxidative stress–diabetic retinopathy and combined oxidative stress–proliferative vitreoretinopathy protein–protein interaction network were used to perform the KEGG pathway enrichment analysis to explore their functions in the human body. The objective of this open-source online application is to offer functional annotation for lengthy lists of target genes and proteins [44].

2.4 Cell culture of ARPE-19 cells

The ARPE-19 human retinal pigment epithelial cell line was grown in DMEM/F12 with 10% FBS and antibiotic penicillin (ThermoFisher) at 37 °C, 5% CO₂ in a 60-mm cell culture dish (Corning, Tewksbury, MA). Trypsin-ethylenediamine tetraacetic acid (trypsin–EDTA; ThermoFisher) was used to detach cells. Different concentrations of either only-H₂O₂, only-TGFβ₂, or H₂O₂ and TGFβ₂ together were administered to the cells. Untreated cells were used as a control for the experiment.

2.5 Cytotoxicity assay

By using the MTT (3-(4,5-Dimethylthiazol-2-yl)-2,5-diphenyltetrazoliumbromide) test, the vitality of ARPE-19 cells was evaluated [45]. In 96-well plates, 1 × 10⁴ cells of the cells were plated in each well. For 12 h, cells were starved in a serum-free medium. Following that, cells were incubated for 24 h with various doses of only-H₂O₂, only-TGFβ₂, and their combinations. TGFβ₂ (1–10 ng/ml) and H₂O₂ (10–1000 μM) final concentrations were produced in a serum-free medium. Following treatment, the cells undergo a 4-h of incubation with 0.5 mg/ml MTT reagent. The formazans were then dissolved in 100 μl of dimethyl sulfoxide (DMSO) at 37 °C, and the absorbance was measured with a microplate reader (Bio-Tek Epoch microplate spectrophotometer, Vermont, USA) at 570 nm. Results were expressed as a percentage of cells that survived, with the control considered as 100%. The cell viability was calculated as described previously by Shukal and coworkers [46].

2.6 Cell migration assay

The ARPE-19 cells were grown in 12 well plates (Corning, NY) at a density of 3 × 10⁵ cells per well until they reached 95 percent confluency. For 12 h before the treatment, cells were serum starved. With the help of a 200 μl tip, a wound was made in the monolayer of cells. To prevent any interruptions to data collection, the detached cells were eliminated using a phosphate-buffered saline (PBS) wash (ThermoFisher). For 24 h, cells were exposed to treatments of only-H₂O₂, only-TGFβ₂ alone, and their combinations. Cells were observed under an inverted microscope (Zeiss, Germany) and 10 photographs were taken from each well using a 5X objective lens at 0 h and after completion of treatment duration of 24 h. Images were analyzed for wound length using ImageJ software (V1.45 NIH, Bethesda, MD, USA) according to the formula described previously by Shukal and colleagues [46].

2.7 RT-PCR, cDNA synthesis, and mRNA expression

As previously noted, the culture of ARPE-19 was carried out up to 75–80% confluency. Cells were treated with just H₂O₂, solely TGF₂, and their mixtures for 24 h after serum starvation. After the course of treatment was complete, RNA was isolated using Trizol reagent (Life Technologies, Waltham, MA, USA) in accordance with the manufacturer's instructions, and 1 g of the isolated RNA was used for cDNA synthesis using Versa cDNA synthesis kit (ThermoFisher, USA) following the manufacturer's instructions. SYBR green master mix (Roche, USA) was used to quantify the gene's expression under the

Table 1 List of primers for quantitative real-time PCR

Target Gene	Forward primer(5'→3')	Reverse primer (5'→3')	PCR fragment length	Gene bank accession number
FN1	GAGCCGGGCATTGACTATGA	ACAAGAAGGAAGACTCAGTTAATGT	138	NM_054034.3
ZO-1	CTACAAGCCTCGGGTTCCT	GGAACCCCGTTCACCATGA	302	NM_001267560.2
N-Cadherin	ATGTGCATGAAGGACAGCCT	TGGAAAGCTTCTCACGGCAT	140	NM_001792.5
E-Cadherin	GCTGGACCGAGAGAGTTTCC	CAAAATCCAAGCCCGTGGTG	155	NM_001317184.2
MMP9	CATCCGGCACCTCTATGGTC	CATCGTCCACCGACTCAAA	270	NM_004994.3
α-SMA	CAGCCAAGCACTGTCAGGAAT	CACCATCACCCCTGATGTC	182	NM_001613.4
Pax6	TCTTGCCCTCAGTTTCCTCC	GCCGCACTTACTTGATAGG	139	NM_001398480.1
RPE65	ATGTGGCCAGGACTCTTTG	GGTCTCTGTGCAAGCGTAGT	316	NM_000329.3
β-catenin	ACACAGGCAATAGGCCTCAA	CGCGTTCTCGAGTACCAGTT	162	NM_001281495.2
S100A4	TTGGTGCTTCTGAGATGTGGG	TTGTCCCTGTTGCTGTCCAA	270	NM_019554.3

manufacturer's instructions on a LightCycler II, Roche, USA. Table 1 describes the list of primers. The results of mRNA expression were calculated by $2^{-\Delta\Delta C_t}$ value by using GAPDH as a housekeeping gene [47].

2.8 Immunofluorescence observation

ARPE-19 cells were plated on coverslips in twelve well culture plates at 75–80% confluence. After treatment duration, coverslips were briefly washed using PBS (ThermoFisher). Cells were fixed in 4% paraformaldehyde (PFA) prepared in phosphate buffer saline (PBS) for 5–6 min. Cells were permeabilized by TritonX-100 in PBS (0.5%) for 30 min at 37 °C. Cells were blocked with 1% bovine serum albumin (BSA, ThermoFisher) in PBS. Cells were exposed to the primary antibody (dilution of 1:100) overnight at 4 °C (Table 2). The blank samples were also processed similarly except for the use of a primary antibody. Then cells were washed with Tween-20 in PBS (0.1%) three times. Cells were exposed to a secondary anti-mouse antibody tagged with Alexa Fluor488 or an anti-rabbit antibody tagged with Alexa Fluor 546 (Dilution 1:100) for 45 min at 37 °C. Then coverslips were washed five times with PBST and counterstained with 4',6-diamidino-2-phenylindole (DAPI) (Sigma), mounted in 1,4-diazabicyclo [2.2.2] octane (DABCO), and observed under the microscope (Zeiss, Germany). Photographs were taken with a charge-coupled device (CCD) camera (Cohu).

2.9 Western blotting

In six-well plates, ARPE-19 cells were plated and allowed to reach 75–80% confluence before being used in western blotting assays. Following the completion of the treatment duration, the cells were rinsed in cold PBS, and the plate was maintained frozen. Cells were harvested using the 1X sample buffer. After a quick

sonication, the cell lysate was centrifuged at 12,000 g for 10 min at 4 °C. The amount of total protein was measured using the BCA protein assay kit. In Bis-Tris gradient gels (ThermoFisher), the same quantity of protein was loaded into each well. The gels were then subjected to further electrophoresis (100 V) until the markers were well separated. Following that, proteins were transferred using a transfer buffer to the nitrocellulose membrane. Blotting was followed by blocking (5% BSA) and a primary antibody incubation at 4 °C for an overnight period while rotation. After being exposed to an anti-rabbit or anti-mouse antibody that had been horseradish peroxidase (HRP)-tagged for an hour at 37 °C, the membrane was then washed with tris-buffered saline with 0.1% Tween® 20 detergent (TBST), and bands were seen using chemiluminescence ECL substrate (BioRad). The images were captured using a gel doc system, and band intensities were calculated using ImageJ software (version 1.45, NIH, Bethesda, Maryland, USA). Results expressed as band intensities divided by GAPDH, where GAPDH served as the housekeeping gene.

2.10 Total glutathione estimation

The total glutathione was measured by the method of Rahman et al., 2007 based on the principle that 5,5'-dithiobis (2-nitrobenzoic acid) (DTNB, Ellman's reagent) reacts with all thiol-containing substances [48]. After completion of the treatment duration, cells were processed immediately after taking from the cell culture and further, all the procedure was carried out over the ice bath. Cells were taken in a known amount of phosphate buffer (0.1 M, pH 7.4) and sonicated for two rounds of 5 s, centrifuged at 12,000 g, 10 min at 4 °C. The resultant supernatant was pipette carefully used further for the enzymatic and estimation. The total 200 µl reaction

Table 2 List of antibodies

Antibody	Supplier	Catalogue #	Working concentration
ZO1	Cell signaling technology, USA	(#5406S)	1:1000
FN1	Cell signaling technology, USA	(#26836S)	1:1000, for IF* 1:100
β-actin	Cell signaling technology, USA	(#4967)	1:1000

*Immunofluorescence

volume which consists of 120 μl of DTNB: GR (60:60 v/v mixture), 60 μl β-NADPH, and 20 μl sample aliquots then immediately readings were taken at 412 nm for every 30 s in a total of 120 s. The system devoid of samples was considered blank. The total GSH is expressed as micromole per milligram of protein. The change in absorbance was measured at 412 nm. The concentration of glutathione was calculated by the linear regression method based on

the glutathione standard. The concentration of total glutathione is expressed as μM/mg protein. The BCA protein assay kit was used for total protein quantification.

2.11 Statistical analysis

Graphs were made using GraphPad Prism software (version 5.01). Data are presented as the means ± SEM. The analysis of variance (ANOVA) was utilized to find the difference between the groups. Statistical significance was set at *p* < 0.05. All experiments were repeated independently at least seven times.

3 Results

3.1 Network pharmacology and gene ontology analysis

A total of 428 oxidative stress, 646 diabetic retinopathy, 180 proliferative vitreoretinopathy-associated genes, and 300 glutathione-associated proteins were identified from GeneCards and DisGeNET databases. These identified potential genes were used to construct their protein–protein interaction networks using the STRING database. The resultant protein–protein interaction networks of oxidative stress, diabetic retinopathy, and proliferative vitreoretinopathy showed 424 nodes/2122 edges, 123 nodes/534 edges, and 170 nodes/244 edges respectively by eliminating unconnected nodes. Additionally, the combined oxidative stress-diabetic retinopathy, oxidative stress-proliferative vitreoretinopathy, and oxidative stress-glutathione protein–protein interaction networks were developed to explore the connection between them which showed that the protein–protein interaction networks network model possessed 123 nodes/534 edges, 33 nodes/77 edges, and 38 nodes/76 edges respectively (Fig. 1A–C).

To illustrate the effect of oxidative stress-associated proteins in diabetic retinopathy as well as proliferative vitreoretinopathy, the proteins of combined oxidative stress and diabetic retinopathy, protein–protein interaction networks were submitted to the DAVID web server to execute the KEGG pathway enrichment analysis. The results of the KEGG pathway enrichment analysis demonstrated that oxidative stress-associated proteins play a critical role in the development of

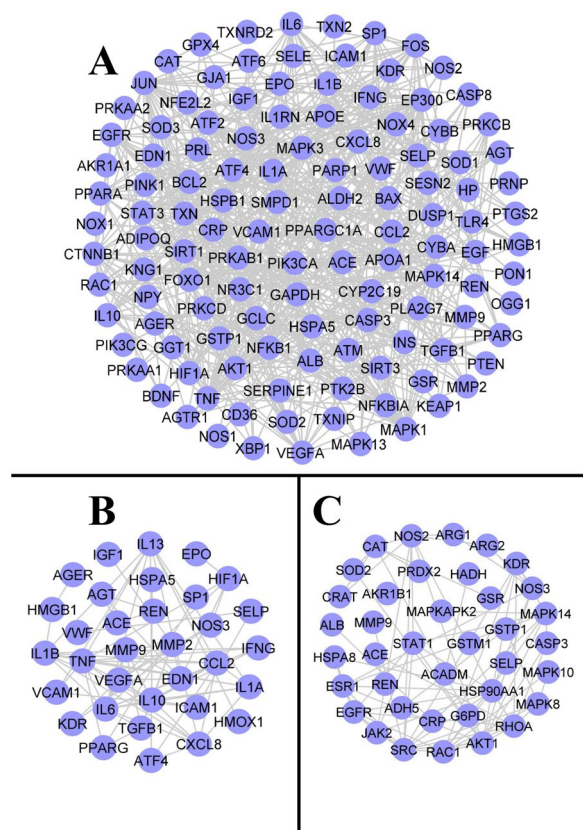


Fig. 1 Combined oxidative stress-diabetic retinopathy protein–protein interactions network (1-A). Combined oxidative stress-proliferative vitreoretinopathy protein–protein interactions network (1-B). Combined diabetic retinopathy-glutathione protein–protein interactions network (1-C). The constructed combined oxidative stress-diabetic retinopathy with 123 nodes and 534 edges. Nodes represent a protein and edges represent the connection between two proteins

Table 3 KEGG pathway enrichment analysis of combined oxidative stress (OS)-diabetic retinopathy (DR), OS-proliferative vitreoretinopathy (PVR) and OS-glutathione PPI network

Pathway ID	Description	DR		PVR		Glutathione	
		Gene count	p value	Gene count	p value	Gene count	p value
hsa04066	HIF-1 signaling pathway	25	7.2e ⁻²³	9	6.5e ⁻⁹	4	1.1e ⁻²
hsa04668	TNF signaling pathway	25	1.2e ⁻²¹	9	1.5e ⁻⁸	6	1.1e ⁻⁴
hsa04068	FoxO signaling pathway	25	3.4e ⁻¹⁹	4	2.2e ⁻²	7	1.7e ⁻⁵
hsa04151	PI3K-Akt signaling pathway	25	7.2e ⁻¹⁰	8	6.9e ⁻⁴	7	3.6e ⁻³
hsa04010	MAPK signaling pathway	22	4e ⁻¹⁰	5	2.6e ⁻²	10	2.8e ⁻⁶
hsa04620	Toll-like receptor signaling pathway	18	5.8e ⁻¹³	4	7.4e ⁻²	6	7.4e ⁻⁵
hsa04660	T cell receptor signaling pathway	14	5.4e ⁻⁹	3	7.4e ⁻²	5	9.7e ⁻⁴
hsa04370	VEGF signaling pathway	14	8.5e ⁻¹²	3	3.1e ⁻²	7	1.5e ⁻⁷
hsa04915	Estrogen signaling pathway	15	4.3e ⁻¹⁰	5	9.4e ⁻³	8	1.6e ⁻⁶
hsa04064	NF-kappa B signaling pathway	11	1.1e ⁻⁶	5	5.8e ⁻³	–	–
hsa04630	JAK-STAT signaling pathway	10	5.2e ⁻⁴	5	3.8e ⁻⁴	4	3.2e ⁻²
hsa04350	TGF-β signaling pathway	7	2.3e ⁻³	4	6.2e ⁻³	–	–

diabetic retinopathy as well as proliferative vitreoretinopathy through regulating signaling pathways such as HIF-1, tumor necrosis factor (TNF), FoxO, PI3K-Akt, mitogen-activated protein kinase (MAPK), Toll-like receptor, T-cell receptor, vascular endothelial growth factor (VEGF), Estrogen, nuclear factor kappa B (NF-kappa B), Janus kinase/signal transducer and activator of transcription signaling pathway (Jak-STAT) and TGF-β (Table 3). In addition, in silico analysis suggested the involvement of potential target proteins of glutathione are associated with oxidative stress by targeting HIF-1, TNF, FoxO, PI3K-Akt, MAPK, Toll-like receptor, T-cell receptor, VEGF, Estrogen, and Jak-STAT signaling pathways.

3.2 Effect of H₂O₂ and TGFβ2 on the Survival of ARPE-19 cells

ARPE-19 cells were exposed to different concentrations of H₂O₂ (Fig. 2) at 10, 20, and 30 μM H₂O₂, there was no significant cell death (at 10 μM $p < 0.001$, at 20 μM $p < 0.001$, and 30 μM, $p < 0.05$). At 40 μM H₂O₂, there was very little effect but after 40 μM, there was a reduction in the survival of cells as H₂O₂ concentration of increased ($p < 0.001$ for all concentrations above 40 μM). TGFβ2 treatment on ARPE-19 cells for 24 h showed a non-significant effect on cell survival (from 1 to 10 ng/ml TGFβ2). The simultaneous treatment of TGFβ2 and H₂O₂ was dependent on the concentration of H₂O₂. Treatment of H₂O₂ at 10, 25 μM, and 100 μM along with 10 ng/ml TGFβ2 showed less cell death compared to that of similar concentration only-H₂O₂ treated cells. However, a higher concentration of H₂O₂

(400 μM) along with 10 ng/ml TGFβ2 showed significantly reduced cell survival compared to that of a similar concentration of only-H₂O₂ treated cells. Based on the above results, we have selected 10 ng/ml TGFβ2 and 10, 25, 100, and 400 μM H₂O₂ for further analysis.

3.3 Effect of H₂O₂ and TGFβ2 on the migration of ARPE-19 cells

Exposure of only-TGFβ2 led to elongated cells compared to that of untreated cells while only-H₂O₂ does not show any cell elongation. The morphology of cells in H₂O₂ along with TGFβ2 treated cells showed elongation (Fig. 3). The wound-healing assay was performed to assess the effect of H₂O₂ on the migration of ARPE-19 cells. The ARPE-19 cells were treated with either TGFβ2 (10 ng/ml) or H₂O₂ (10, 25, 100, 400 μM) and their combinations for 24 h. Figure 2 shows the representative images of the ARPE-19 wound healing response. TGFβ2 (10 ng/ml) along with H₂O₂-exposure increased the wound healing response of cells compared to the untreated groups (Fig. 2). H₂O₂ at 10, 25, and 100 μM showed higher wound closure compared to that of the untreated group. However, 400 μM H₂O₂ led to reduced wound closure than untreated cells. Based on the above results, we have selected 25 μM and 100 μM H₂O₂ for further evaluation.

3.4 Effect of H₂O₂ and TGFβ2 on the expression of epithelial–mesenchymal transition markers

The effects of H₂O₂ and TGFβ2 is evaluated at mRNA, cellular, and protein levels. The results of mRNA expression are shown in Fig. 4. We have used zonula occludens-1 (ZO1), E-cadherin, β-catenin, and Pax6 as epithelial/RPE markers. H₂O₂ exposure at 25 μM did not

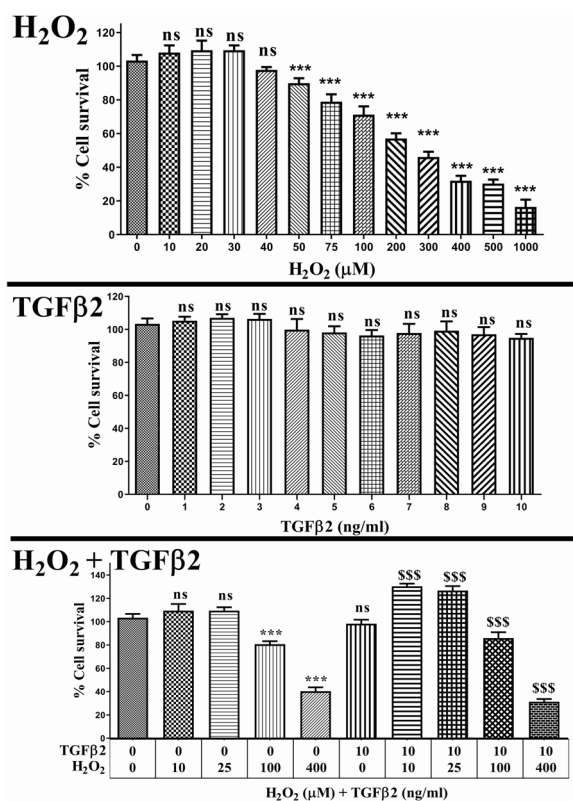


Fig. 2 Effects of H₂O₂ and TGFβ₂ on the survival of ARPE-19 cells. Exposure of H₂O₂ after 40 μM, the OS-dependent reduction in cell survival observed compared to control (*** = $p < 0.001$). The Exposure of only-TGFβ₂ (1–10 ng/ml) showed the non-significant change in cell survival compared to the untreated control. There was no cell death observed when the treatment of TGFβ₂ (10 ng/ml) when it given simultaneously with H₂O₂ (10, 25 μM and 100 μM) compared to that of similar concentrations of only-H₂O₂ treated cells. However, at higher concentrations of H₂O₂ (400 μM) reduced the survival observed compared 10 ng/ml TGFβ₂ treated cells. $n = 7$ for each group. Data represented by mean \pm SEM as a percentage to that of untreated cells. All TGFβ₂ and H₂O₂ concentrations tested are compared with untreated cells and shown with ns, non-significant, * = $p < 0.05$, ** = $p < 0.01$, and *** = $p < 0.001$. The combination of TGFβ₂ and H₂O₂ are compared with similar concentration of H₂O₂ and represented as \$ = $p < 0.05$, \$\$ = $p < 0.01$, and \$\$\$ = $p < 0.001$ for 10 ng/ml TGFβ₂

alter the expression of ZO1, E-cadherin, and β-catenin ($p < 0.05$) and increased expressions of Pax6 ($p < 0.01$) compared to untreated control groups. H₂O₂ exposure at 100 μM reduced the expression of ZO1 ($p < 0.05$), E-cadherin ($p < 0.05$), and β-catenin ($p < 0.01$). TGFβ₂ at 10 ng/ml reduced the expression of all epithelial/RPE markers compared to that of untreated cells. The simultaneous treatment of TGFβ₂ and H₂O₂ furthermore significantly reduced the expression of all epithelial/RPE markers compared to that of respective concentrations of only-H₂O₂. We have used fibronectin, alpha-smooth muscle

actin (α-SMA), S100A4, and matrix metalloproteinase 9 (MMP9) as a marker of epithelial–mesenchymal transition. The simultaneous treatment of TGFβ₂ (10 ng/ml) and H₂O₂ (25 μM and 100 μM) elevated the expression of all epithelial–mesenchymal transition markers compared to that of respective concentrations of only-H₂O₂.

The effect of only-TGFβ₂, only-H₂O₂, and a combination of H₂O₂ and TGFβ₂ on the expression of fibronectin is shown in Fig. 5. Immunofluorescence staining revealed that fibronectin was expressed both intracellularly as a diffused stain in the cytoplasm and extracellularly as a speckle of fibers. Fibronectin expression was found significantly increased in the treatment of TGFβ₂ (10 ng/ml) and H₂O₂ (25 μM and 100 μM) compared to the respective concentration of only-H₂O₂ and compared to that of untreated cells.

The results of protein expressions shown in Fig. 6. We have used ZO1 as epithelial and fibronectin as a mesenchymal marker. The combined effect of TGFβ₂ and H₂O₂ on ZO1 remained less than that of the respective concentration of only-H₂O₂ treated cells. The fibronectin protein levels found increased by the simultaneous treatment of TGFβ₂ (10 ng/ml) along with both 25 and 100 μM H₂O₂ treatment compared to that of untreated cells (# = $p < 0.05$, ## = $p < 0.01$, and ### = $p < 0.001$).

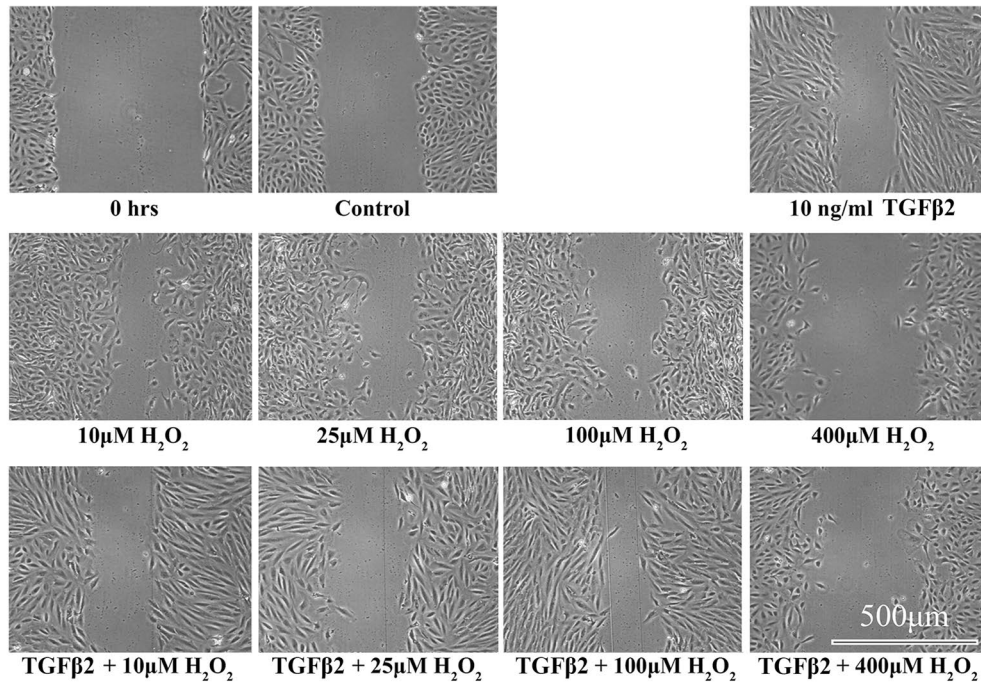
3.5 Effects on total glutathione content of TGFβ₂ and H₂O₂ treated ARPE-19 cells

The results suggest the involvement of oxidative stress in the epithelial–mesenchymal transition of Retinal pigment epithelium cells (Fig. 7). The treatment of only-TGFβ₂ (10 ng/ml) showed downregulated glutathione compared to untreated control cells (** = $p < 0.01$). The treatment of only-H₂O₂ treated cells (25 μM and 100 μM H₂O₂) also showed decreased glutathione (\$ = $p < 0.05$, ** = $p < 0.01$). However, the simultaneous treatment of TGFβ₂ (10 ng/ml) along with H₂O₂ (25 μM and 100 μM H₂O₂) showed significantly decreased glutathione compared to untreated control and only-TGFβ₂ treated ARPE-19 cells (*** = $p < 0.05$, ### = $p < 0.01$).

4 Discussion

Network pharmacology is a computational approach to investigating the interactions of multiple proteins in various therapeutic conditions [49]. The results of the current study indicate that 123 (OS-DR) and 33 (OS-PVR) oxidative stress-associated proteins have a significant impact on the epithelial–mesenchymal transition of retinal pigment epithelium cells. KEGG pathway enrichment analysis further demonstrated that oxidative stress-associated proteins can activate pathways including PI3K-Akt, MAPK, and TGFβ-signaling. The literature further supports our findings by suggesting that ocular cells,

Wound healing



Wound closure

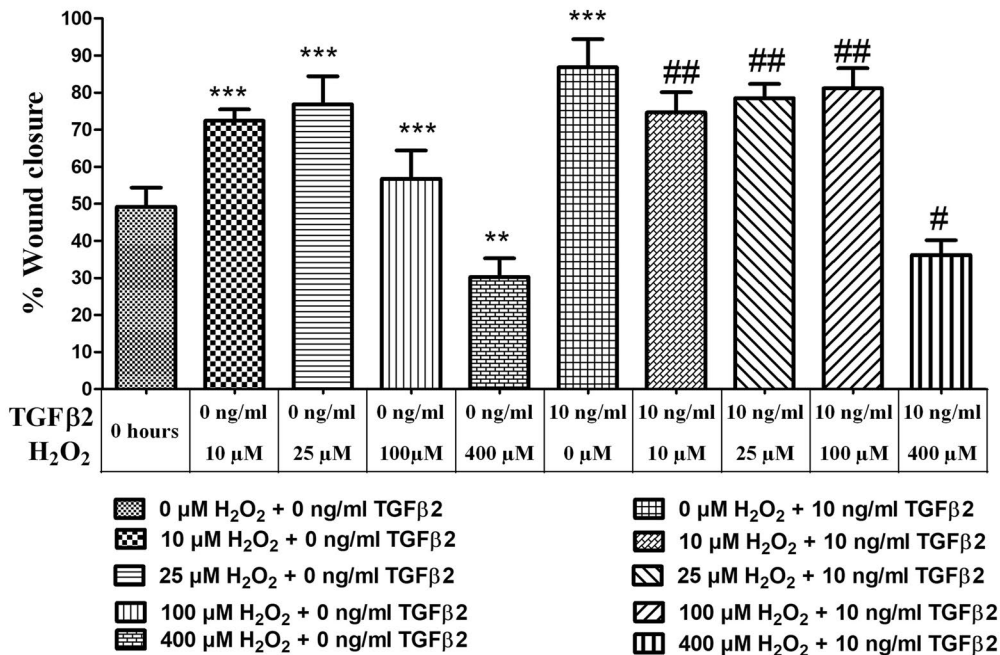


Fig. 3 Effects of H₂O₂ and TGFβ2 on the wound healing of ARPE-19 cells. Exposure of TGFβ2 led to elongated cells and increased wound closure compared to that of untreated control cells. High concentration of H₂O₂ at 400 μM reduced the migration of cells and hence reduced the wound closure. The simultaneous treatment of H₂O₂ (10 μM, 25 μM, 100 μM) along with TGFβ2(10 ng/ml), the increased wound closure was observed compared to untreated and only-H₂O₂ treated cells and showed elongated cells. However, at 400 μM H₂O₂ along with 10 ng/ml TGFβ2, the wound closure was reduced than that of only H₂O₂. n = 7 for each group. Data represented by mean ± SEM as a percentage to that of untreated cells. All TGFβ2 and H₂O₂ concentrations tested are compared with untreated control cells and shown with ** = p < 0.01, and *** = p < 0.001. The combination of TGFβ2 and H₂O₂ was compared with a similar concentration of only H₂O₂ and represented as # = p < 0.05, and ## = p < 0.01

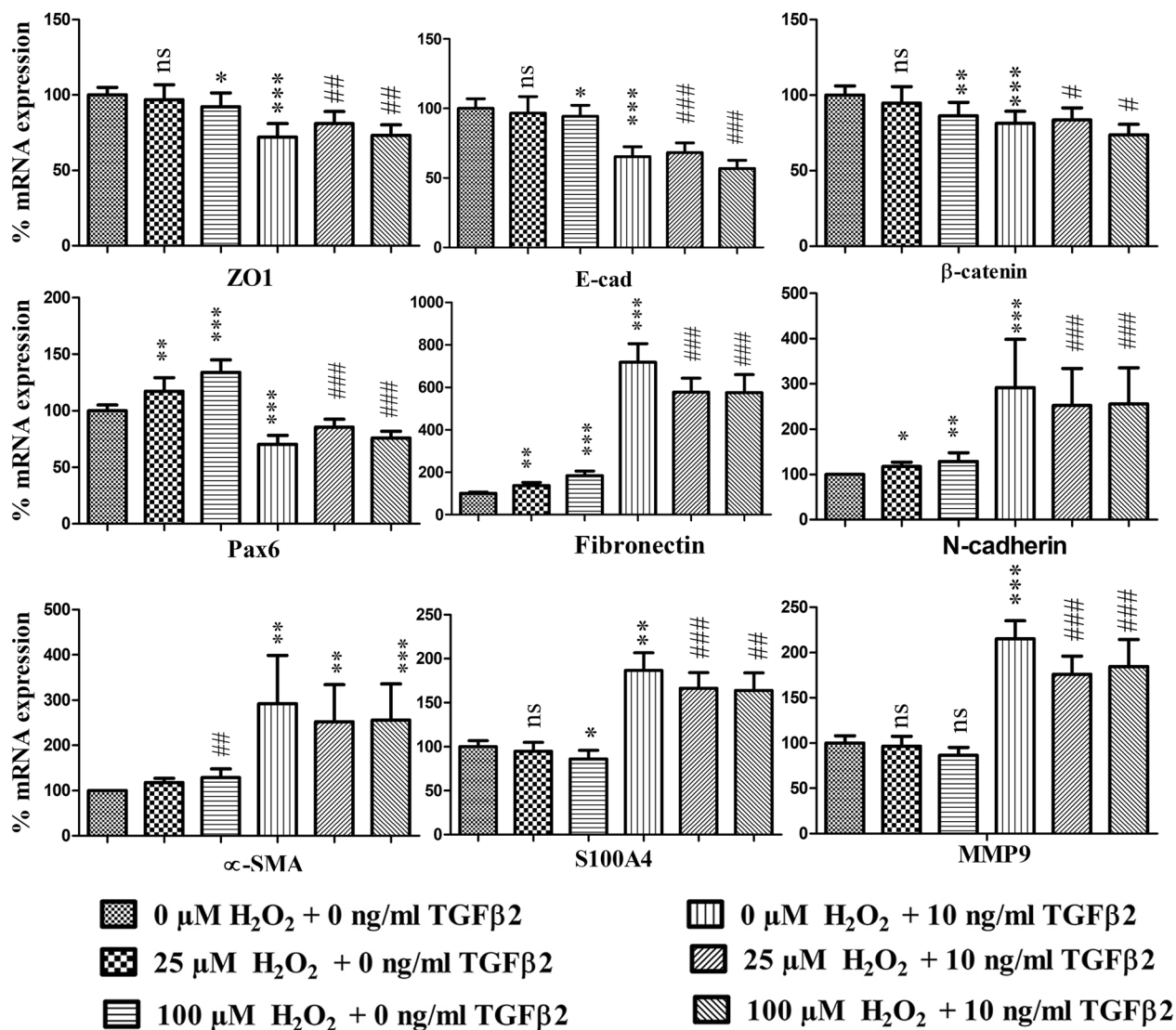


Fig. 4 Effects of H₂O₂ and TGFβ₂ on the expression of various epithelial and epithelial-mesenchymal transition markers at mRNA level in the ARPE-19 cells. The mRNA expression of epithelial markers ZO1, E-cadherin and β-catenin reduced with the simultaneous exposure H₂O₂ and TGFβ₂ compared to untreated control cells. Similarly, the Pax6 mRNA expression also reduced compared to untreated cells. The combined effect of H₂O₂ with TGFβ₂ increased expression of mesenchymal-markers (fibronectin, N-cadherin, α-SMA, S100A4, MMP9) compared to that of only-H₂O₂. n = 7 for each group. Data are represented as a percentage of control as mean ± SEM. H₂O₂ alone and TGFβ₂ alone exposures were compared with the untreated cells and shown with ns = non-significant, * = p < 0.05, ** = p < 0.01, and *** = p < 0.001. The combination of TGFβ₂ and H₂O₂ were compared with similar concentration of only-H₂O₂ and represented as # = p < 0.05, ## = p < 0.01, and ### = p < 0.001

particularly retinal pigment epithelium cells, undergo epithelial-mesenchymal transition predominantly through non-canonical TGFβ signaling, which includes the PI3K-Akt and MAPK/Erk signaling pathways. Hypoxia and inflammatory pathways also contribute to the execution of the epithelial-mesenchymal transition process in retinal pigment epithelium cells [50–52]. It is not known, however, how oxidative stress triggers SMAD and MEK/ERK signaling to increase TGFβ-mediated

EMT. However, since TGFβ is stimulated by oxidative stress, SMAD activation may be brought on by TGFβ.

The reduced cell survival observed in the current study might be attributed to the increased oxidative stress in cells where the antioxidant capacity of retinal pigment epithelium cells is largely suppressed. Our findings of decreased viability of ARPE-19 cells are consistent with previous research in response to subtoxic concentrations (50–300 μM) of H₂O₂ [24, 53]. Oxidative stress has

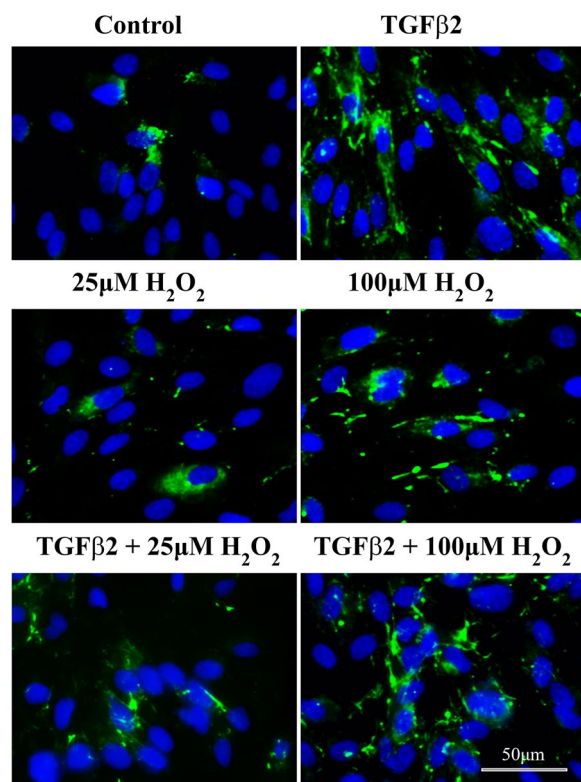


Fig. 5 Effects of H_2O_2 and TGF β 2 on fibronectin of the ARPE-19 cells (Immunofluorescence aspect). TGF β 2 exposure led to elongation of cell nuclei and increased expression of fibronectin. However, the combined exposure of H_2O_2 and TGF β 2 showed more significantly increased expression of fibronectin compared to untreated and only- H_2O_2 treated ARPE-19 cells

been shown to cause cell–cell dissociation, which may be required to initiate epithelial–mesenchymal transition [21, 54, 55]. α -SMA is an active isoform that is expressed specifically in myofibroblasts and is considered a critical marker for epithelial–mesenchymal transition [56]. According to the findings of a current study, the combined treatment of H_2O_2 and TGF β 2 upregulates the expression of α -SMA. Additionally, fibronectin is a key component of the extracellular matrix of drusen in ophthalmopathies [57]. Results of the current study show that the level of fibronectin increases several-fold after the simultaneous treatment of TGF β 2 and H_2O_2 . Our understanding suggests that the increase in fibronectin could be due to the induction of epithelial–mesenchymal transition in ARPE-19 cells under the influence of oxidative stress. Other mesenchymal markers, S100A4 and MMP9, are also upregulated epithelial markers E-cadherin, ZO1, Pax6, and β -catenin are downregulated as a result of the effects of oxidative stress. However, when only- H_2O_2 is exposed, Pax6 mRNA levels were found to be upregulated while S100A4 and MMP9 levels were

downregulated, indicating the epithelial–mesenchymal transition of cells.

Earlier studies show that TGF β is capable of raising ROS levels by suppressing the production of antioxidant enzymes and lowering the amounts of antioxidant enzymes [58]. Taken together with the results of the current study, the effect of only- H_2O_2 has a variable effect on the expression of various epithelial markers as well as mesenchymal markers, but combined treatments result in increased mesenchymal expression and decreased epithelial marker expression. As a result, the presence of TGF β 2 is required epithelial–mesenchymal transition of ARPE-19 cells; additionally, the presence of H_2O_2 enhances the effect of TGF β 2 and leads to a more significant increase in the expression of epithelial–mesenchymal transition. In the current study, we used total glutathione as an indicator of oxidative stress and our results indicate that the combined treatment of TGF β 2 and H_2O_2 resulted in a significant decrease in glutathione. In support of our results earlier study conducted by Wei and coworkers on lens epithelial cells showed that a low glutathione level is a key event in promoting epithelial–mesenchymal transition [20]. Furthermore, in addition to the liver, lungs, and lens epithelial cells, low glutathione levels have been seen in a number of human fibrotic diseases [20, 59–61].

In the current study, wound closure increased in response to oxidative stress when simultaneous treatment of H_2O_2 and TGF β 2 was given to ARPE-19 cells. Furthermore, the literature suggests that treatment of only- H_2O_2 is insufficient to induce epithelial–mesenchymal transition in cells [62]. Although, it is also suggested that only TGF β 2 treatment is insufficient to cause cell–cell junction dissociations [15]. As a result, the microenvironment containing both H_2O_2 and TGF β 2 appears to be required to induce the epithelial–mesenchymal transition of ARPE-19 cells, and further research is needed to understand the role of glutathione and the complex signaling cascade involved in the activation and induction of epithelial–mesenchymal transition of ARPE-19 cells under oxidative stress microenvironment.

In summary, the current work shows that mild oxidative stress can alter the epithelial–mesenchymal transitions of the retinal pigment epithelium in vitro and *in-silico*. According to this study, antioxidant medication may be used to treat epithelial–mesenchymal transitions of the retinal pigment epithelium. It is important to understand the complex interactions and roles of TGF β 2 and oxidative stress in the initiation, progression, and eventual discovery of potential therapeutics for anti-EMT treatment of epithelial–mesenchymal transitions of retinal pigment epithelium in humans. However, the first limitation of the current study is to elucidate the complex

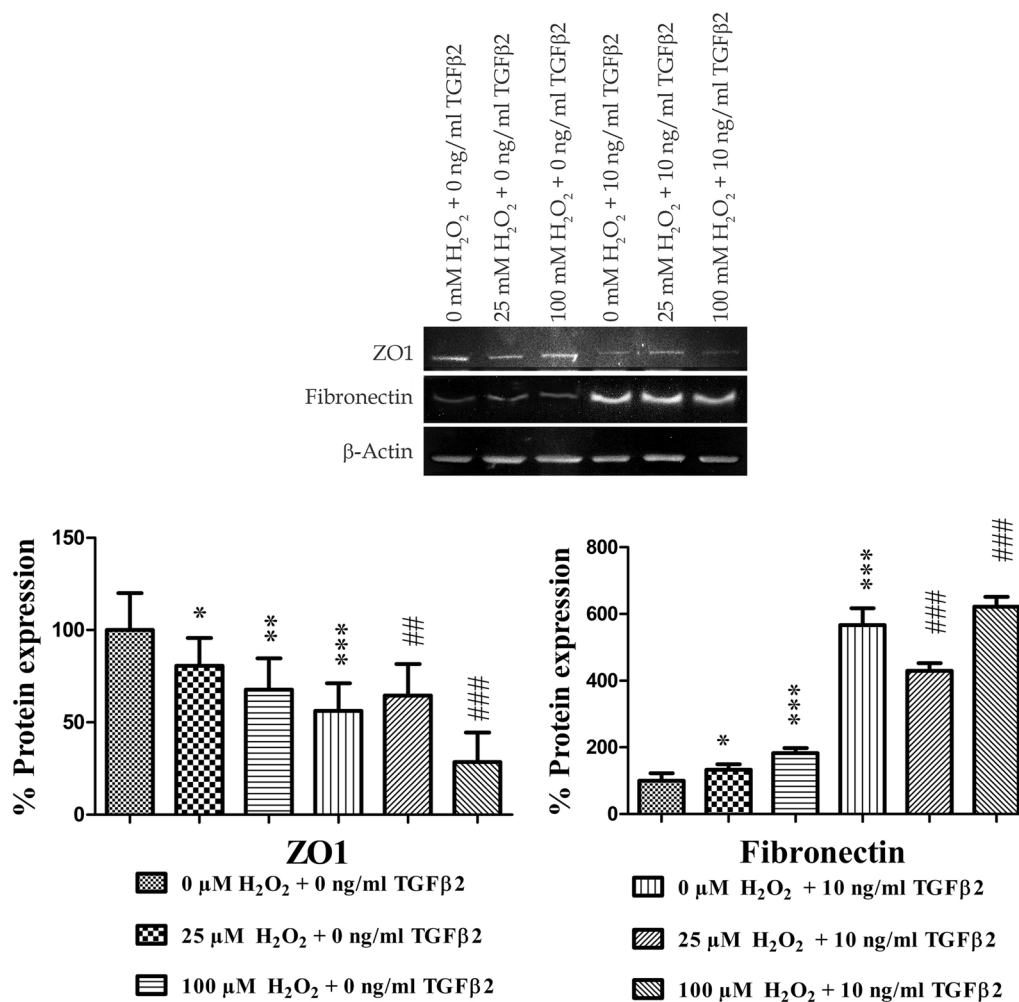


Fig. 6 Effects of H₂O₂ and TGFβ₂ on the expression of epithelial and epithelial–mesenchymal transition markers at the protein level in the ARPE-19 cells. The combined treatment of H₂O₂ and TGFβ₂ showed reduced expression of ZO1 and showed increased expressions of fibronectin compared to untreated ARPE-19 cells and only-H₂O₂ treated cells. n = 5 for each group. Data are represented as a percentage of untreated cells as mean ± SEM. H₂O₂ alone and TGFβ₂ alone exposure were compared with the untreated cells and shown with ns = non-significant, * = p < 0.05, ** = p < 0.01, and *** = p < 0.001. The combination of TGFβ₂ and H₂O₂ compared with a similar concentration of only-H₂O₂ and represented as # = p < 0.05, ## = p < 0.01, and ### = p < 0.001

signaling cascade interplay and roles of TGFβ₂ and oxidative stress in epithelial–mesenchymal transitions of the retinal pigment epithelium. The second limitation is that we only examined ARPE-19 cells in vitro; thus, the aforementioned results need to be confirmed using primary retinal pigment epithelial cells before being further tested in vivo. We currently intend to confirm it at the primary cell line level. The third limitation is that we have only used an in-silico (bioinformatics) method to clarify the significance of signaling cascades in the epithelial–mesenchymal transition of retinal pigment epithelial cells; however, we also need to validate this at the protein level using western blotting. The fourth limitation is that we only represented a 24-h exposure time since it is

more physiologically relevant. It should be investigated to examine the effects of the treatment after 48 and 72 h. The fifth limitation is that glutathione was the only antioxidant enzyme used in the current study as a measure of oxidative stress; however, other antioxidant enzymes such as superoxide dismutase (SOD), catalase (CAT), and glutathione peroxidase (GPx) also need to be assessed for alterations.

5 Conclusions

Taken together, the results of the present study show that, the presence of hydrogen peroxide enhances TGFβ₂-induced epithelial–mesenchymal transition of human retinal pigment epithelial cell line, ARPE-19 cells.

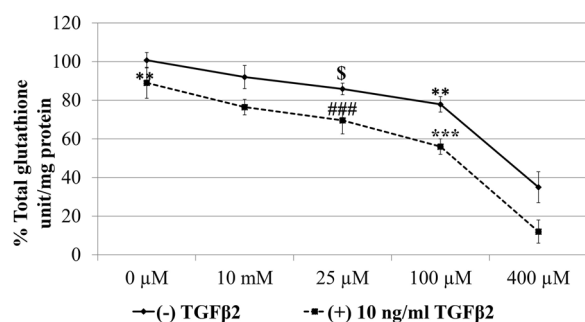


Fig. 7 Estimation of total glutathione of TGFβ2 and H₂O₂ treated ARPE-19 cells. The results suggested the involvement of oxidative stress in the epithelial–mesenchymal transition of retinal pigment epithelium cells. The treatment of only-TGFβ2 (10 ng/ml) showed downregulated glutathione compared to untreated control cells (**=*p* < 0.01). The treatment of only-H₂O₂ (25 μM and 100 μM H₂O₂) also showed decreased glutathione (\$=*p* < 0.05, **=*p* < 0.01) compared to untreated control cells. However, the simultaneous treatment of TGFβ2 (10 ng/ml) and H₂O₂ (25 μM and 100 μM H₂O₂) showed significantly decreased glutathione compared to untreated control and only-TGFβ2 treated ARPE-19 cells (***=*p* < 0.001, ###=*p* < 0.001)

Abbreviations

ARPE-19	A human retinal pigment epithelial cell
BCA	Bicinchoninic acid assay
BSA	Bovine serum albumin
cDNA	Complementary DNA
DABCO	1,4-Diazabicyclo [2.2.2] octane
DAPI	4',6-Diamidino-2-phenylindole
DAVID	Database annotation, visualization, and integrated discovery
DMEM	Dulbecco's modified eagle medium
DMSO	Dimethyl sulfoxide
DR	Diabetic retinopathies
DTNB	5,5'-Dithiobis (2-nitrobenzoic acid)
ECL	Electrochemiluminescence
EDTA	Ethylenediamine tetraacetic acid
EMT	Epithelial–mesenchymal transition
FBS	Foetal bovine serum
FoxO	Forkhead box O
GSH	Glutathione
H ₂ O ₂	Hydrogen peroxide
HIF-1	Hypoxia-inducible factor
HRP	Horseshoe peroxidase
Jak-STAT	Janus kinase/signal transducer and activator of transcription signaling pathway
KEGG	Kyoto encyclopaedia of genes and genomes
MAPK	Mitogen-activated protein kinase
MMP9	Matrix metalloproteinase 9
MTT	3-(4,5-Dimethylthiazol-2-yl)-2,5-diphenyltetrazoliumbromide
NF-kappa B	Nuclear factor kappa B
PBS	Phosphate buffered saline
PCR	Polymerase chain reaction
PDR	Proliferative diabetic retinopathy
PI3K-Akt	Phosphoinositide-3-kinase
PPI	Protein–protein interaction
PVR	Proliferative vitreoretinopathy
ROS	Reactive oxygen species
RPE cells	Retinal pigment epithelial cells
SDS	Sodium dodecyl sulfate
SEM	Standard error of means
TBS	Tris-buffered saline
TBST	Tris-buffered saline with 0.1% Tween® 20 detergent
TGFβ2	Transforming growth factors-β2

TNF	Tumor necrosis factor
VEGF	Vascular endothelial growth factor
ZO1	Zonula occludens-1
α-SMA	Alpha-smooth muscle actin

Acknowledgements

Not applicable.

Author contributions

Data curation, Formal analysis, Investigation, Methodology, Software, Validation, Writing—original draft by BG, PR, PM, BP and KJ. KJ and AV formulated the hypothesis. BG, PM, BP and PR were responsible for conducting the experiments. All authors have contributed in the writing of the manuscript.

Funding

Not applicable.

Availability of data and materials

Not applicable.

Declarations

Ethics approval and consent to participate

Not applicable.

Consent for publication

Not applicable.

Competing interests

The authors have declared that they have no competing interests.

Author details

¹Department of Zoology, Biomedical Technology, Human Genetics, and WBC, School of Sciences, Gujarat University, Ahmedabad, Gujarat 380009, India. ²Iladevi Cataract and IOL Research Center, Gurukul Road, Memnagar, Ahmedabad, Gujarat 380054, India. ³Department of Life Sciences, School of Sciences, Gujarat University, Ahmedabad, Gujarat 380009, India.

Received: 16 March 2023 Accepted: 7 September 2023

Published online: 07 November 2023

References

- Panda-Jonas S, Jonas JB, Jakobczyk-Zmija M (1996) Retinal pigment epithelial cell count, distribution, and correlations in normal human eyes. *Am J Ophthalmol* 121:181–189. [https://doi.org/10.1016/S0002-9394\(14\)70583-5](https://doi.org/10.1016/S0002-9394(14)70583-5)
- Zhou M, Geathers JS, Grillo SL, Weber SR, Wang W, Zhao Y, Sundstrom JM (2020) Role of epithelial–mesenchymal transition in retinal pigment epithelium dysfunction. *Front Cell Dev Biol* 8:501. <https://doi.org/10.3389/fcell.2020.00501>
- Gelat B, Rathaur P, Malaviya P, Patel B, Trivedi K, Johar K, Gelat R (2022) The intervention of epithelial–mesenchymal transition in homeostasis of human retinal pigment epithelial cells: a review. *J Histotechnol* 45:148–160. <https://doi.org/10.1080/01478885.2022.2137665>
- Rizzolo LJ (2007) Development and Role of tight junctions in the retinal pigment epithelium. *Int Rev Cytol* 258:195–234. [https://doi.org/10.1016/S0074-7696\(07\)58004-6](https://doi.org/10.1016/S0074-7696(07)58004-6)
- Xia T, Rizzolo LJ (2017) Effects of diabetic retinopathy on the barrier functions of the retinal pigment epithelium. *Vision Res* 139:72–81. <https://doi.org/10.1016/j.visres.2017.02.006>
- Narimatsu T, Ozawa Y, Miyake S, Kubota S, Hirasawa M, Nagai N, Shimamura S, Tsubota K (2013) Disruption of cell–cell junctions and induction of pathological cytokines in the retinal pigment epithelium of light-exposed mice. *Investig Ophthalmol Vis Sci* 54:4555–4562. <https://doi.org/10.1167/iovs.12-11572>
- Acloque H, Adams MS, Fishwick K, Bronner-Fraser M, Nieto MA (2009) Epithelial–mesenchymal transitions: the importance of changing cell state

- in development and disease. *J Clin Invest* 119:1438–1449. <https://doi.org/10.1172/JCI38019>
8. Kalluri R, Weinberg RA (2009) The basics of epithelial–mesenchymal transition. *J Clin Invest* 119:1420–1428. <https://doi.org/10.1172/JCI39104>
 9. Iizuka D, Sasatani M, Barcellos-Hoff MH, Kamiya K (2017) Hydrogen peroxide enhances tgf-mediated epithelial-to-mesenchymal transition in human mammary epithelial mcf-10a cells. *Anticancer Res* 37:987–995. <https://doi.org/10.21873/anticancer.11408>
 10. Zhang Y, Wang K, Pan J, Yang S, Yao H, Li M, Li H, Lei H, Jin H, Wang F (2020) Exosomes mediate an epithelial–mesenchymal transition cascade in retinal pigment epithelial cells: implications for proliferative vitreoretinopathy. *J Cell Mol Med* 24:13324–13335. <https://doi.org/10.1111/jcmm.15951>
 11. Kalluri R, Neilson EG (2003) Epithelial–mesenchymal transition and its implications for fibrosis. *J Clin Invest* 112:1776–1784. <https://doi.org/10.1172/JCI200320530>
 12. Liang CM, Tai MC, Chang YH, Chen YH, Chen CL, Lu DW, Chen JT (2011) Glucosamine inhibits epithelial-to-mesenchymal transition and migration of retinal pigment epithelium cells in culture and morphologic changes in a mouse model of proliferative vitreoretinopathy. *Acta Ophthalmol* 89:505–514. <https://doi.org/10.1111/j.1755-3768.2011.02147.x>
 13. Xu S, Zhan M, Wang J (2017) Epithelial-to-mesenchymal transition in gallbladder cancer: from clinical evidence to cellular regulatory networks. *Nat Publ Gr*. <https://doi.org/10.1038/cddiscovery.2017.69>
 14. Nisticò P, Bissell MJ, Radisky DC (2012) Epithelial–mesenchymal transition: general principles and pathological relevance with special emphasis on the role of matrix metalloproteinases. *Cold Spring Harb Perspect Biol*. <https://doi.org/10.1101/cshperspect.a011908>
 15. Yang IH, Lee JJ, Wu PC, Kuo HK, Kuo YH, Huang HM (2020) Oxidative stress enhanced the transforming growth factor- β 2-induced epithelial–mesenchymal transition through chemokine ligand 1 on ARPE-19 cell. *Sci Rep* 10:1–10. <https://doi.org/10.1038/s41598-020-60785-x>
 16. Tamiya S, Kaplan HJ (2016) Role of epithelial–mesenchymal transition in proliferative vitreoretinopathy. *Exp Eye Res* 142:26–31. <https://doi.org/10.1016/j.exer.2015.02.008>
 17. Ghosh S, Shang P, Terasaki H, Stepicheva N, Hose S, Yazdankhah M, Weiss J, Sakamoto T, Bhutto IA, Xia S, Zigler JS, Kannan R, Qian J, Handa JT, Sinha D (2018) A role for β A3/A1-crystallin in type 2 EMT of RPE cells occurring in dry age-related macular degeneration. *Investig Ophthalmol Vis Sci* 59:AMD104–AMD113. <https://doi.org/10.1167/iovs.18-24132>
 18. Ishikawa K, He S, Terasaki H, Nazari H, Zhang H, Spee C, Kannan R, Hinton DR (2015) Resveratrol inhibits epithelial–mesenchymal transition of retinal pigment epithelium and development of proliferative vitreoretinopathy. *Sci Rep*. <https://doi.org/10.1038/srep16386>
 19. Ung et al (2017) Oxidative stress and reactive oxygen species: a review of their role in ocular disease. *Clin Sci* 131:2865–2883. <https://doi.org/10.1042/CS20171246>
 20. Wei Z, Caty J, Whitson J, Zhang AD, Srinivasagan R, Kavanagh TJ, Yan H, Fan X (2017) Reduced glutathione level promotes epithelial–mesenchymal transition in lens epithelial cells via a Wnt/ β -catenin–mediated pathway: relevance for cataract therapy. *Am J Pathol* 187:2399–2412. <https://doi.org/10.1016/j.ajpath.2017.07.018>
 21. Inumaru J, Nagano O, Takahashi E, Ishimoto T, Nakamura S, Suzuki Y, Niwa SJ, Umezawa K, Tanihara H, Saya H (2009) Molecular mechanisms regulating dissociation of cell–cell junction of epithelial cells by oxidative stress. *Genes Cells* 14:703–716. <https://doi.org/10.1111/j.1365-2443.2009.01303.x>
 22. Mateos MV (2015) Inflammation and oxidative stress in retinal diseases: the role of intracellular signaling in the retinal pigment epithelium. *Int J Ophthalmol Clin Res*. <https://doi.org/10.23937/2378-346x/1410033>
 23. Cano M, Wang L, Wan J, Barnett BP, Ebrahimi K, Qian J, Handa JT (2014) Oxidative stress induces mitochondrial dysfunction and a protective unfolded protein response in RPE cells. *Free Radic Biol Med* 69:1–14. <https://doi.org/10.1038/jid.2014.371>
 24. Angulo Daniela F (2015) Intracellular redox status and cell death Induced by H₂O₂ in a human retinal epithelial cell line (ARPE-19). *Am J Biosci*. <https://doi.org/10.11648/j.ajbio.20150303.15>
 25. Kim MH, Chung J, Wook Yang J, Chung SM, Kwag NH, Yoo JS (2003) Hydrogen peroxide-induced cell death in a human retinal pigment epithelial cell line, ARPE-19. *Korean J Ophthalmol* 17:19–28. <https://doi.org/10.3341/kjo.2003.17.1.19>
 26. Sen CK, Khanna S, Gordillo G, Bagchi D, Bagchi M, Roy S (2002) Oxygen, oxidants, and antioxidants in wound healing: an emerging paradigm. *Ann N Y Acad Sci*. <https://doi.org/10.1111/j.1749-6632.2002.tb02920.x>
 27. Sjölie AK, Klein R, Porta M, Orchard T, Fuller J, Parving HH, Bilous R, Aldington S, Chaturvedi N (2011) Retinal microaneurysm count predicts progression and regression of diabetic retinopathy. Post-hoc results from the DIRECT Programme. *Diabet Med* 28:345–351. <https://doi.org/10.1111/j.1464-5491.2010.03210.x>
 28. Shukal D, Bhadresha K, Shastri B, Mehta D, Vasavada A, Johar K Sr (2020) Dichloroacetate prevents TGF β -induced epithelial–mesenchymal transition of retinal pigment epithelial cells. *Exper Eye Res* 197:108072
 29. Cao Q, Deji QZ, Liu YJ, Ye W, Zhaba WD, Jiang Q, Yan F (2019) The role of mechanical stretch and TGF- β 2 in epithelial–mesenchymal transition of retinal pigment epithelial cells. *Int J Ophthalmol* 12:1832–1838. <https://doi.org/10.18240/ijo.2019.12.03>
 30. Akhurst RJ, Hata A (2012) Targeting the TGF β signalling pathway in disease. *Nat Rev Drug Discov* 11:790–811. <https://doi.org/10.1038/nrd3810>
 31. Krstić J, Trivanović D, Mojsilović S, Santibanez JF (2015) Transforming growth factor-beta and oxidative stress interplay: implications in tumorigenesis and cancer progression. *Oxid Med Cell Longev*. <https://doi.org/10.1155/2015/654594>
 32. Liu R, FRB KP (2010) and medicine, undefined 2010, Oxidative stress and glutathione in TGF- β -mediated fibrogenesis, Elsevier. (n.d.). <https://www.sciencedirect.com/science/article/pii/S0891584909005681>. Accessed 31 July 2023
 33. Wu WS (2006) The signaling mechanism of ROS in tumor progression. *Cancer Metastasis Rev* 25:695–705. <https://doi.org/10.1007/s10555-006-9037-8>
 34. Parapuram SK, Chang B, Li L, Hartung RA, Chalam KV, Nair-Menon JU, Hunt DM, Hunt RC (2009) Differential effects of TGF β and vitreous on the transformation of retinal pigment epithelial cells. *Investig Ophthalmol Vis Sci* 50:5965–5974. <https://doi.org/10.1167/iovs.09-3621>
 35. Mony S, Lee SJ, Harper JF, Barwe SP, Langhans SA (2013) Regulation of Na, K-ATPase β 1-subunit in TGF- β 2-mediated epithelial-to-mesenchymal transition in human retinal pigmented epithelial cells. *Exp Eye Res* 115:113–122. <https://doi.org/10.1016/j.exer.2013.06.007>
 36. Tosi GM, Caldi E, Neri G, Nuti E, Marigliani D, Baiocchi S, Traversi C, Cevenini G, Tarantello A, Fusco F, Nardi F, Orlandini M, Galvagni F (2017) HTRA1 and TGF- β 1 concentrations in the aqueous humor of patients with neovascular age-related macular degeneration. *Investig Ophthalmol Vis Sci* 58:162–167. <https://doi.org/10.1167/iovs.16-20922>
 37. Saika S (2006) TGF β pathobiology in the eye. *Lab Invest* 86:106–115. <https://doi.org/10.1038/labinvest.3700375>
 38. Shu DY, Lovicu FJ (2017) Myofibroblast transdifferentiation: the dark force in ocular wound healing and fibrosis. *Prog Retin Eye Res* 60:44–65. <https://doi.org/10.1016/j.preteyeres.2017.08.001>
 39. Liu RM, Desai LP (2015) Reciprocal regulation of TGF- β and reactive oxygen species: a perverse cycle for fibrosis. *Redox Biol* 6:565–577. <https://doi.org/10.1016/j.redox.2015.09.009>
 40. Stelzer G, Rosen N, Plaschkes I, Zimmerman S, Twik M, Fishilevich S, Iny Stein T, Nudel R, Lieder I, Mazor Y, Kaplan S, Dahary D, Warshavsky D, Guan-Golan Y, Kohn A, Rappaport N, Safran M, Lancet D (2016) The GeneCards suite: from gene data mining to disease genome sequence analyses. *Curr Protoc Bioinforma* 2016:1.30.1–1.30.33. <https://doi.org/10.1002/cpbi.5>
 41. Piñero J, Ramírez-Anguita JM, Saüch-Pitarch J, Ranzano F, Centeno E, Sanz F, Furlong LI (2020) The DisGeNET knowledge platform for disease genomics: 2019 update. *Nucleic Acids Res* 48:D845–D855. <https://doi.org/10.1093/nar/gkz1021>
 42. Szklarczyk D, Gable AL, Nastou KC, Lyon D, Kirsch R, Pyysalo S, Doncheva NT, Legeay M, Fang T, Bork P, Jensen LJ, von Mering C (2021) The STRING database in 2021: customizable protein-protein networks, and functional characterization of user-uploaded gene/measurement sets. *Nucleic Acids Res* 49:D605–D612. <https://doi.org/10.1093/nar/gkaa1074>
 43. Shannon P, Markiel A, Ozier O, Baliga NS, Wang JT, Ramage D, Amin N, Schwikowski B, Ideker T (2003) Cytoscape: a software Environment for integrated models of biomolecular interaction networks. *Genome Res* 13:2498–2504. <https://doi.org/10.1101/gr.1239303>
 44. Jiao X, Sherman BT, Huang DW, Stephens R, Baseler MW, Lane HC, Lempicki RA (2012) DAVID-WS: a stateful web service to facilitate gene/

- protein list analysis. *Bioinformatics* 28:1805–1806. <https://doi.org/10.1093/bioinformatics/bts251>
45. Mosmann T (1983) Rapid colorimetric assay for cellular growth and survival: application to proliferation and cytotoxicity assays. *J Immunol Methods* 65:55–63. [https://doi.org/10.1016/0022-1759\(83\)90303-4](https://doi.org/10.1016/0022-1759(83)90303-4)
 46. Shukal D, Bhadresha K, Shastri B, Mehta D, Vasavada A, Johar K (2020) Dichloroacetate prevents TGF β -induced epithelial–mesenchymal transition of retinal pigment epithelial cells. *Exp Eye Res.* <https://doi.org/10.1016/j.exer.2020.108072>
 47. Livak KJ, Schmittgen TD (2001) Analysis of relative gene expression data using real-time quantitative PCR and the 2- $\Delta\Delta$ CT method. *Methods* 25:402–408. <https://doi.org/10.1006/meth.2001.1262>
 48. Rahman I, Kode A, Biswas SK (2007) Assay for quantitative determination of glutathione and glutathione disulfide levels using enzymatic recycling method. *Nat Protoc* 1:3159–3165. <https://doi.org/10.1038/nprot.2006.378>
 49. Chandran U, Mehendale N, Patil S, Chaguturu R, Patwardhan B (2017) Network pharmacology. *Innov Approac Drug Discov Ethnopharmacol Syst Biol Holist Target.* <https://doi.org/10.1016/B978-0-12-801814-9.00005-2>
 50. Parvathaneni K, Grigsby JG, Betts BS, Tsin AT (2013) Estrogen-induced retinal endothelial cell proliferation: possible involvement of pigment epithelium-derived factor and phosphoinositide 3-kinase/mitogen-activated protein kinase pathways. *J Ocul Pharmacol Ther* 29:27–32. <https://doi.org/10.1089/jop.2011.0252>
 51. Bayan N, Yazdanpanah N, Rezaei N (2022) Role of toll-like receptor 4 in diabetic retinopathy. *Pharmacol Res.* <https://doi.org/10.1016/j.phrs.2021.105960>
 52. Min J, Zeng T, Roux M, Lazar D, Chen L, Tudzarova S (2021) The role of HIF1 α -PFKFB3 pathway in diabetic retinopathy. *J Clin Endocrinol Metab* 106:2505–2519. <https://doi.org/10.1210/clinem/dgab362>
 53. Yang Wang Z, Jun Shen L, Tu LL, Ning Hu D, Liu GY, Lou Zhou Z, Lin Y, Chen LH, Qu J (2009) Erythropoietin protects retinal pigment epithelial cells from oxidative damage. *Free Radic Biol Med* 46:1032–1041. <https://doi.org/10.1016/j.freeradbiomed.2008.11.027>
 54. Yang X, Chung JY, Rai U, Esumi N (2018) Cadherins in the retinal pigment epithelium (RPE) revisited: P-cadherin is the highly dominant cadherin expressed in human and mouse RPE in vivo. *PLoS ONE* 13:1–20. <https://doi.org/10.1371/journal.pone.0191279>
 55. Chen X, Yan H, Chen Y, Li G, Bin Y, Zhou X (2021) Moderate oxidative stress promotes epithelial–mesenchymal transition in the lens epithelial cells via the TGF- β /Smad and Wnt/ β -catenin pathways. *Mol Cell Biochem* 476:1631–1642. <https://doi.org/10.1007/s11010-020-04034-9>
 56. He H, Kuriyan AE, Su CW, Mahabole M, Zhang Y, Zhu YT, Flynn HW, Parel JM, Tseng SCG (2017) Inhibition of proliferation and epithelial mesenchymal transition in retinal pigment epithelial cells by heavy chain-hyaluronan/pentraxin 3. *Sci Rep.* <https://doi.org/10.1038/srep43736>
 57. Biasella F, Plössl K, Karl C, Weber BHF, Friedrich U (2020) Altered protein function caused by AMD-associated variant rs704 links vitronectin to disease pathology. *Investig Ophthalmol Vis Sci.* <https://doi.org/10.1167/IOVS.61.14.2>
 58. Liu RM, Gaston Pravia KA (2010) Oxidative stress and glutathione in TGF- β -mediated fibrogenesis. *Free Radic Biol Med* 48:1–15. <https://doi.org/10.1016/j.freeradbiomed.2009.09.026>
 59. Roum JH, Buhl R, McElvaney NG, Borok Z, Crystal RG (1993) Systemic deficiency of glutathione in cystic fibrosis. *J Appl Physiol* 75:2419–2424. <https://doi.org/10.1152/jappl.1993.75.6.2419>
 60. Bianchi G, Bugianesi E, Ronchi M, Fabbri A, Zoli M, Marchesini G (1997) Glutathione kinetics in normal man and in patients with liver cirrhosis. *J Hepatol* 26:606–613. [https://doi.org/10.1016/S0168-8278\(97\)80426-6](https://doi.org/10.1016/S0168-8278(97)80426-6)
 61. Deger Y, Yur F, Ertekin A, Mert N, Dede S, Mert H (2007) Protective effect of α -tocopherol on oxidative stress in experimental pulmonary fibrosis in rats. *Cell Biochem Funct* 25:633–637. <https://doi.org/10.1002/cbf.1362>
 62. Felton VM, Borok Z, Willis BC (2009) N-acetylcysteine inhibits alveolar epithelial–mesenchymal transition. *Am J Physiol Lung Cell Mol Physiol.* <https://doi.org/10.1152/ajplung.00009.2009>

Publisher's Note

Springer Nature remains neutral with regard to jurisdictional claims in published maps and institutional affiliations.

Submit your manuscript to a SpringerOpen[®] journal and benefit from:

- Convenient online submission
- Rigorous peer review
- Open access: articles freely available online
- High visibility within the field
- Retaining the copyright to your article

Submit your next manuscript at ► [springeropen.com](https://www.springeropen.com)